Transient Stabilization Improvement of Induction Generator Based Power System using Robust Integral Linear Quadratic Gaussian Approach

Faisal R. Badal‡, Subrata K. Sarker and Sajal K. Das

Department of Mechatronics Engineering, Rajshahi University of Engineering & Technology, Rajshahi-6204, Bangladesh

(faisalrahman1312@gmail.com, skshuvo138008@gmail.com and das.k.sajal@gmail.com)

‡Corresponding Author: Faisal R. Badal, Rajshahi-6204, Tel: +8801763130652,

Email: faisalrahman1312@gmail.com

Received: 01.06.2019 Accepted:15.06.2019

Abstract- Interconnected power system consisting of a number of power generation units are able to fulfil the demand of electricity throughout the world. A safe and reliable operation of interconnected power system is possible when all the generators remain at synchronism state. Stability problem arises when the damping torque of these generators is reduced due to the effect of different uncertainties, faults and dynamic loads. The result of insufficient damping torque may deviate the speed of the generators and produce unsafe operation of power system due to the loss of stability and robustness of terminal voltage and rotor angle. In this paper, a novel integral linear-quadratic Gaussian (ILQG) controller is designed to regulate the oscillation of the power system for increasing stability and robustness. The better performance of the proposed controller is ensured by comparing it with the linear-quadratic regulator (LQR) and the linear-quadratic Gaussian (LQG) controllers. The comparison results ensure the optimum performance of the proposed controller against uncertainties and fault as compared to the LQR and LQG controller.

Keywords: Single machine infinite bus, Integral linear-quadratic Gaussian control, Speed regulation, Rotor angle regulation, Terminal voltage regulation.

1. Introduction

The electric demand over the world is increasing rapidly. A reliable and efficient solution to meet the growing demand of this electricity is the innovation of interconnected power system consisting of a number of generators [1], [2]. It provides a better and reliable supply of power and becomes exoteric with the development of the world [3], [4]. It receives energy from different sources and ensures reliability to the consumers. Wind turbine, solar, hydropower etc. are integrated to the main grid to provide additional energy throughout the year. It controls the system frequency and managing the tie transfer between utility regions and increases the reliability against disturbances [5]-[7].

The reliability and safe operation of the power system can be hampered due to fluctuation of the power. Power fluctuation occurs due to the unknown loads and faults [8][9]. The inertia and synchronising force may be hampered and system outages may be increased while operating the power system with renewable energies [10]. Again, the large demand of the electrical power may produce stress on the grid and hamper its stability [11]-[14]. The dynamics of the stressed power system is complex [15]. It exhibits nonlinear nature depending on the system structure, loads and unknown fault [16]. Although, the initial oscillation of the performances is quite small with the change of system loads, a large change of loads or disturbance may make it a disaster for the power system.

Induction machines and the components of power system also effect its performance. The machines of the interconnected power system must be synchronized for an unbreakable power supply [17]-[19]. Low damping torque, transmission line fault and unknown loads are responsible to hamper the synchronism of the machines and produce unsafe operation [20].

The synchronism of the power system are related to two control stability such as, (i) steady state and (ii) transient stability [21]. At small change of loads, power system stability is the static stability while the other one is responsible to synchronous all the machines of the power

system. The transient stability is a function of both operational conditions and disturbances which is controlled by automatic voltage regulator (AVR) [22].

A weak control of the power system against different disturbances and faults increases the oscillations and deviations of its performances. The effects of the disturbances on the power system may increase the control challenge of rotor angle, speed and transient stability of the terminal voltage of the generators [23]. At synchronous state, any variation of the generator speed is minimized by damping torque to regain the synchronous speed of the generators. Dynamic loads, weak control of AVR, dynamic variation of the system parameters can reduce the restoring torque of the machine and cause instability [12].

The regulation of the damping torque of the generators to regain the operating equilibrium against different uncertainties is the main aim. A bounded system is able to withstand the disturbances and back to the equilibrium point. Controlling of each generator speed is the tendency to take the damping torque within equilibrium point to enhance the control performance of terminal voltage and rotor angle [24]-[27].

A number of control techniques have been proposed for a better control of different deviations of power system by controlling damping torque of the generators. Proportional-plus-Integral-plus-Derivative (PID) is the largely used industrial controller has been designed to enhance the stability of the interconnected power system [18], [28]-[30]. The simple design and implementation of the PID controller efficiently reduces the deviations of speed and rotor angle of the generator. Low bandwidth and robustness against uncertainties are the limitations of the PID controller.

Power system stabilizer (PSS) technique minimizes the limitations of the PID controller. It provides better protection of the power system against different uncertainties by restoring it [31], [32]. This control algorithm is deigned based on the control principle of fuzzy logic and sliding mode controller. Alone the fuzzy logic controller minimizes the effect of uncertainty and hazy of the power system. The low robustness against un-modelled loads is the limitation of this control approach. Sliding mode controller samples the sensor output whose objective function is minimized by fuzzy logic controller that are responsible for robust performance against different uncertainties.

Static synchronous compensator (STATCOM) has been proposed to control the stability of the power system. This control algorithm damps out the low-frequency oscillation produced by uncertainties and loads faults. This controller is designed based on the seeker optimization algorithm (OA) [33]. This algorithm is used to optimize the compensator parameter to minimize the objective function. STATCOM is also designed based on the cultural algorithm (CA) to tune the stabilizer parameter [34]. This controller faces optimization problem. For proper voltage regulation, distributed static synchronous compensator (DSTATCOM) has been proposed [35] by linearizing the the system order based on partial feedback linearization approach.

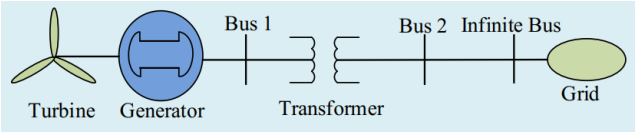

Fig. 1. Illusion of SMIB Structure.

To overcome the limitation of STATCOM controller, unified power flow controller (UPFC) has been proposed [36] that is a FACT device to improve the damping torque, active and reactive power. This control approach is designed based on electromagnetic transient algorithm. UPFC is difficult to use for power system having a large number of generation units.

The design of model predictive controller (MPC) has been proposed to enhance the stability of power system [8], [37], [38]. This control approach is designed with UPFC for better controlling of active and reactive power and damping torque. It has the ability to predict the control output and provides optimal function for desired performance. This control algorithm exhibits high gain and phase margin. The bandwidth of MPC against different loads and uncertainties is quite low.

The control structure of linear-quadratic regulator (LQR) has been proposed to reduce the deviations of the performances and increase the stability of the power system [39]-[41]. The controller design is based on linearization approach of mean value theorem. It provides a fast and accurate response which is optimal with respect to operating cost. The cost function of this optimal controller is minimized by the control algorithm of Algebraic Riccati Equation (ARE). Its performance may be harmed by dynamic loads.

A novel integral linear-quadratic Gaussian (ILQG) controller design is presented in this work for deviation control of the performances of single machine infinite bus (SMIB). The motivation for designing the ILQG controller over the LQR and the LQG controller is its ability to track the reference signal and robustness against the plant uncertainty. The design of the controller is done by augmenting the plant dynamics with an integrator which reduces the oscillation and provides the fast transient response as compared to the LQR and the LQG controller. The proposed ILQG controller minimizes H_2 norm of the objective function which results in high gain of the controller. The aim of this paper is to guarantee the stable operation of the SMIB for different uncertainties. The controller performances are tested using Matlab. The results ensure that the ILQG controller shows the minimum deviation for rotor angle, speed and terminal voltage which confirms the better performance as compared to the LQR and the LQG controller.

The remaining paper is arranged as follows: System modelling and controller design is presented in Section 2 and 3. The performance investigation of the controllers is carried out in Section 4. Section 5 contains the conclusion of this paper.

2. Power System Modelling

An interconnected power system consists of a number of generators that are used to produce electricity from renewable and non-renewable energy source. A constant dynamic behavior of all generators is essential for safe and better performance. This large number of generation units and components increase the complexity of interconnected power system to investigate its performances. Single machine infinite bus (SMIB) is the possible solution to analysis the control performance of one generation unit of power system that exhibits similar performance of all generation units connected to the power system. The basic structure of SMIB is presented in Fig. 1. The capacity of the infinite bus is large enough i.e infinite whose voltage and frequency remain constant.

A set of mechanical and electrical model are used to represents the dynamics of SMIB [16], [17], [42]. The overall nonlinear mechanical model to represent the generator of SMIB can be written as,

$$\begin{aligned}\dot{\tilde{\delta}} &= \tilde{\omega}_0(\tilde{\omega} - 1) \\ \dot{\tilde{\omega}} &= \frac{1}{2H}(-D\tilde{\omega} - P_M + P_E)\end{aligned} \tag{1}$$

Where $\tilde{\delta}$, H and D represent the rotor angle, inertia and damping constant of the generator. $\tilde{\omega}_0$ and $\tilde{\omega}$ are the synchronous and rotor speed. P_M and P_E are the supplied mechanical power to and delivered electrical power from the generator.

The nonlinear electrical dynamics model representation for generator are,

$$\begin{aligned}\dot{\tilde{E}}_q &= \frac{1}{T_d}(-E_q + \tilde{E}_{fd}) \\ \dot{\tilde{E}}_{fd} &= \frac{1}{T_a}[K_a(V_{ref} - V_t) - \tilde{E}_{fd}]\end{aligned} \tag{2}$$

Where $\tilde{E}_q$, E_q and $\tilde{E}_{fd}$ are the transient voltage, generator voltage and exciter voltage of the generator. K_a and T_a are the exciter gain and time constant. V_{ref} and V_t are the obtained terminal voltage from and applied reference voltage to the generator. The algebraic equations for electrical model of the generator can be represented as

$$E_q = \frac{\hat{x}_d}{\hat{\tilde{x}}_d}\tilde{E}_q - (x_d - \tilde{x}_d)\frac{V_s}{\tilde{x}_d}\cos\delta$$

$$I_d = \frac{\tilde{E}_q}{\hat{\tilde{x}}_d} - \frac{V_s}{\tilde{x}_d}\cos\delta$$

$$I_q = \frac{V_s}{\hat{\tilde{x}}_d}\sin\delta$$

$$P_E = \frac{\tilde{E}_q V_s}{\hat{\tilde{x}}_d}\sin\delta$$

$$Q_E = \frac{\tilde{E}_q V_s}{\hat{\tilde{x}}_d}\cos\delta - \frac{V_s^2}{\hat{\tilde{x}}_d}$$

$$V_q = \tilde{E}_q - \tilde{x}_d I_d$$

$$V_d = \tilde{x}_d I_q$$

$$\overline{V}_t = \sqrt{\overline{V}_d^{\,2} + \overline{V}_q^{\,2}}$$

$$\hat{\tilde{x}}_d = \tilde{x}_d + \tilde{x}_T + 0.5\tilde{x}_L$$

$$\hat{x}_d = x_d + \tilde{x}_T + 0.5\tilde{x}_L$$

Where x_d and $\tilde{x}_d$ are the reactance and transient reactance of the generator. $\tilde{x}_T$ and $\tilde{x}_L$ are the transformer and transmission line reactance. I_q and I_d are the generator current alone quadrature- and direct-axis. V_s and Q_E are infinite bus voltage and reactive power.

Now from Eq. (1) and (2), the overall representation of SMIB can be written as,

$$\begin{aligned}\dot{\tilde{\delta}} &= \tilde{\omega}_0(\tilde{\omega} - 1) \\ \dot{\tilde{\omega}} &= \frac{1}{2H}(-D\tilde{\omega} - P_M + \frac{\tilde{E}_q V_s}{\hat{\tilde{x}}_d}\sin\delta) \\ \dot{\tilde{E}}_q &= \frac{1}{T_d}(-\frac{\hat{x}_d}{\hat{\tilde{x}}_d}\tilde{E}_q + (x_d - \tilde{x}_d)\frac{V_s}{\tilde{x}_d}\cos\delta + \tilde{E}_{fd}) \\ \dot{\tilde{E}}_{fd} &= \frac{1}{T_a}[K_a(V_{ref} - \sqrt{(\tilde{E}_q - \tilde{x}_d I_d)^2 + (\tilde{x}_d I_q)^2}) - \tilde{E}_{fd}]\end{aligned} \tag{3}$$

The nonlinear model of SMIB is difficult to analysis. it is essential to convert the nonlinear system into linear to make ease the analysis of the performance of SMIB. A nonlinear time-variant system can be written as,

$$\begin{aligned}\dot{\tilde{x}} &= h(\tilde{x}, u, t) \\ \tilde{y} &= g(\tilde{x}, u, t)\end{aligned}$$

Where $\tilde{x}$, u and $\tilde{y}$ are the system state, input and output vector. h and g are the nonlinear input and output vector

function of the system. When the system does not depend on the time is called time-invariant system that can be represented as

$$\begin{aligned}\dot{\tilde{x}} &= h(\tilde{x},u)\\ \tilde{y} &= g(\tilde{x},u)\end{aligned} \tag{4}$$

For synchronism, let the initial state and input vector at equilibrium point are $\tilde{x}_0$ and u_0, then,

$$\dot{\tilde{x}}_0 = h(\tilde{x}_0,u_0) = 0$$

Any deviation Δ from the equilibrium point makes new state vector $\tilde{x} = \dot{\tilde{x}}_0 + \Delta\tilde{x}$ and input vector $u = \dot{u}_0 + \Delta u$, that are responsible for new state of the system such as,

$$\dot{\tilde{x}} = h[(\dot{\tilde{x}}_0 + \Delta\tilde{x}),(\dot{u}_0 + \Delta u)]$$

With this small deviation, Taylor's series can be used to represent a complete nonlinear system such as,

$$\begin{aligned}\dot{\tilde{x}}_i &= h_i(\tilde{x}_0,u_0) + \frac{\partial h_i(\tilde{x}_0,u_0)}{\partial\tilde{x}_1}\Delta\tilde{x}_1 + \frac{\partial h_i(\tilde{x}_0,u_0)}{\partial\tilde{x}_2}\\ &\Delta\tilde{x}_2 + \ldots + \frac{\partial h_i(\tilde{x}_0,u_0)}{\partial\tilde{x}_n}\Delta\tilde{x}_n + \frac{\partial h_i(\tilde{x}_0,u_0)}{\partial u_1}\Delta u_1 +\\ &\frac{\partial h_i(\tilde{x}_0,u_0)}{\partial u_2}\Delta u_2 + \ldots + \frac{\partial h_i(\tilde{x}_0,u_0)}{\partial u_n}\Delta u_n\end{aligned} \tag{5}$$

Where i = 1, 2, 3, ...n. Since $f_i = (\tilde{x}_0,u_0) = 0$, Eq. (5) can be represented as,

$$\begin{aligned}\Delta\dot{\tilde{x}}_i &= \frac{\partial h_i(\tilde{x}_0,u_0)}{\partial\tilde{x}_1}\Delta\tilde{x}_1 + \frac{\partial h_i(\tilde{x}_0,u_0)}{\partial\tilde{x}_2}\Delta\tilde{x}_2 + \ldots\\ &+ \frac{\partial h_i(\tilde{x}_0,u_0)}{\partial\tilde{x}_n}\Delta\tilde{x}_n + \frac{\partial h_i(\tilde{x}_0,u_0)}{\partial u_1}\Delta u_1 + \frac{\partial h_i(\tilde{x}_0,u_0)}{\partial u_2}\\ &\Delta u_2 + \ldots + \frac{\partial h_i(\tilde{x}_0,u_0)}{\partial u_n}\Delta u_n\end{aligned}$$

and for the output,

$$\begin{aligned}\dot{y}_j &= g_j(\tilde{x}_0,u_0) + \frac{\partial g_j(\tilde{x}_0,u_0)}{\partial\tilde{x}_1}\Delta\tilde{x}_1 + \frac{\partial g_j(\tilde{x}_0,u_0)}{\partial\tilde{x}_2}\\ &\Delta\tilde{x}_2 + \ldots + \frac{\partial g_j(\tilde{x}_0,u_0)}{\partial\tilde{x}_n}\Delta\tilde{x}_n + \frac{\partial g_j(\tilde{x}_0,u_0)}{\partial u_1}\Delta u_1 +\\ &\frac{\partial g_j(\tilde{x}_0,u_0)}{\partial u_2}\Delta u_2 + \ldots + \frac{\partial g_j(\tilde{x}_0,u_0)}{\partial u_n}\Delta u_n\end{aligned} \tag{6}$$

Where j = 1, 2, 3,...n. Since $g_j = (\tilde{x}_0,u_0) = 0$, Eq. (6) can be represented as,

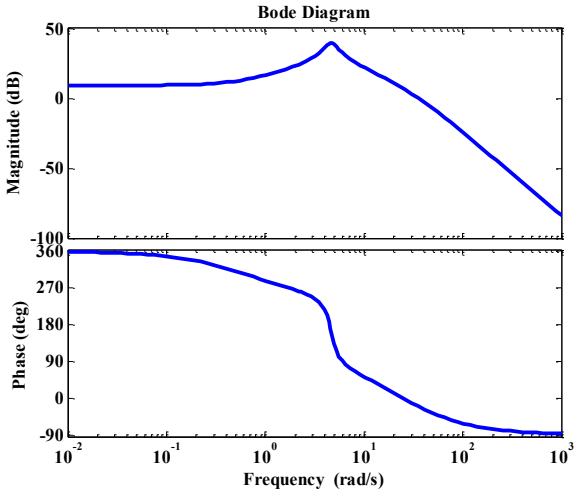

Fig. 2. Bode Diagram of Open-loop System.

$$\begin{aligned}\Delta\dot{y}_j &= \frac{\partial g_j(\tilde{x}_0,u_0)}{\partial\tilde{x}_1}\Delta\tilde{x}_1 + \frac{\partial g_j(\tilde{x}_0,u_0)}{\partial\tilde{x}_2}\Delta\tilde{x}_2 + \ldots\\ &+ \frac{\partial g_j(\tilde{x}_0,u_0)}{\partial\tilde{x}_n}\Delta\tilde{x}_n + \frac{\partial g_j(\tilde{x}_0,u_0)}{\partial u_1}\Delta u_1 + \frac{\partial g_j(\tilde{x}_0,u_0)}{\partial u_2}\\ &\Delta u_2 + \ldots + \frac{\partial g_j(\tilde{x}_0,u_0)}{\partial u_n}\Delta u_n\end{aligned}$$

Therefore, the linearized from of Eq. (4) can be represented as,

$$\begin{aligned}\Delta\dot{\tilde{x}} &= A\Delta\tilde{x} + B\Delta u\\ \Delta y &= C\Delta\tilde{x} + D\Delta u\end{aligned}$$

Where,

$$A = \begin{bmatrix}\frac{\partial h_1}{\partial\tilde{x}_1} & \cdots & \frac{\partial h_n}{\partial\tilde{x}_n}\\ \vdots & \vdots & \vdots\\ \frac{\partial h_n}{\partial\tilde{x}_1} & \cdots & \frac{\partial h_n}{\partial\tilde{x}_n}\end{bmatrix} \quad B = \begin{bmatrix}\frac{\partial h_1}{\partial u_1} & \cdots & \frac{\partial h_n}{\partial u_n}\\ \vdots & \vdots & \vdots\\ \frac{\partial h_n}{\partial u_1} & \cdots & \frac{\partial h_n}{\partial u_n}\end{bmatrix}$$

$$C = \begin{bmatrix}\frac{\partial g_1}{\partial\tilde{x}_1} & \cdots & \frac{\partial g_n}{\partial\tilde{x}_n}\\ \vdots & \vdots & \vdots\\ \frac{\partial g_n}{\partial\tilde{x}_1} & \cdots & \frac{\partial g_n}{\partial\tilde{x}_n}\end{bmatrix} \quad D = \begin{bmatrix}\frac{\partial g_1}{\partial u_1} & \cdots & \frac{\partial g_n}{\partial u_n}\\ \vdots & \vdots & \vdots\\ \frac{\partial g_n}{\partial u_1} & \cdots & \frac{\partial g_n}{\partial u_n}\end{bmatrix}$$

Where A, B, C and D are the state, input, output and transition matrix of a system. There are four state $\tilde{x}$ for SMIB that can be written as,

$$\tilde{x} = \begin{bmatrix}\Delta\tilde{\delta} & \Delta\tilde{\omega} & \Delta\tilde{E}_q & \Delta\tilde{E}_{fd}\end{bmatrix}^T$$

Based on this technique, Eq. (3) can be linearized as,

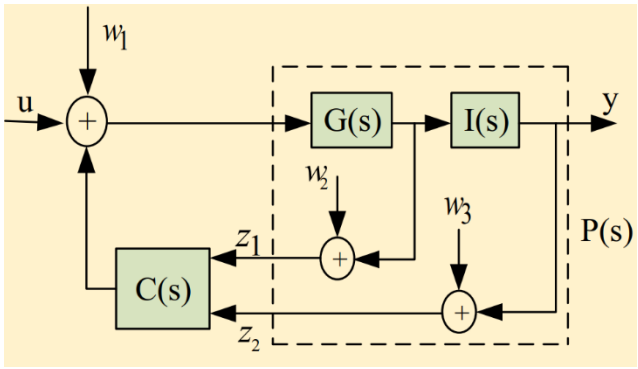

Fig. 3. Closed-loop Structure of SMIB with ILQG Controller.

$$A=\begin{bmatrix} 0 & \tilde{\omega}_0 & 0 & 0 \\ -\frac{K_1}{2H} & -\frac{D}{2H} & -\frac{K_2}{2H} & 0 \\ -\frac{K_4}{T_d} & 0 & -\frac{K_3}{T_d} & \frac{1}{T_d} \\ -\frac{K_A K_5}{T_A} & 0 & -\frac{K_A K_6}{T_A} & -\frac{1}{T_A} \end{bmatrix}, \quad B=\begin{bmatrix} 0 \\ \frac{1}{2H} \\ 0 \\ 0 \end{bmatrix},$$

$$C=\begin{bmatrix} 0 & 1 & 0 & 0 \end{bmatrix}, \quad D=0$$

Where $K_1 - K_6$ can be written as,

$$K_1=\frac{\tilde{E}_q V_s \hat{\tilde{x}}_d}{\cos\delta}-\frac{V_s^2(x_q-\tilde{x}_d)}{\hat{\tilde{x}}_d \hat{x}_d}\cos 2\delta$$

$$K_2=\frac{V_s}{\hat{\tilde{x}}_d}\sin\delta$$

$$K_3=\frac{\hat{x}_d}{\hat{\tilde{x}}_d}$$

$$K_4=\frac{V_s(x_q-\tilde{x}_d)}{\hat{\tilde{x}}_d}\sin\delta$$

$$K_5=\frac{V_s x_q V_{td}}{\hat{x}_q \tilde{V}_t}\cos\delta-\frac{V_s \tilde{x}_d V_{tq}}{\hat{\tilde{x}}_d V_t}\sin\delta$$

$$K_6=\frac{x_T V_{tq}}{\hat{\tilde{x}}_d \tilde{V}_t}$$

Here, V_{td} and V_{tq} are the d and q component of the terminal voltage of the induction machine. The performance of the open-loop frequency domain response is reported in Fig. 2. The peak value of frequency domain is almost 40 dB. The bode diagram shows that the open-loop system has positive gain. According to the control theory, a positive gain system is unstable. The aim of our proposed controller is to make the system stable by reducing the peak value against uncertainties.

3. Design of Proposed Controller

Fig. 3 represents the control structure of ILQG controller [43], [44]. Consider the plant dynamics:

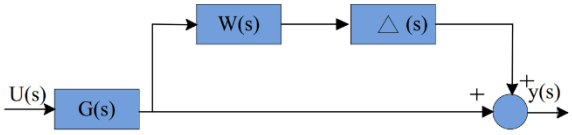

Fig. 4. Block Diagram of Inverse Multiplicative Output Uncertainty

Table 1. Design Parameter Value

LQR Controller	$R=1; Q=1\times10^{-5}$
LQG Controller	$R=1\times10^{-1}; Q=1\times10^{-7};$ $\omega_n=1\times10^{-3}; \omega_d=1\times10^{-4}$
ILQG Controller	$\gamma_1=1\times10^{8}; \gamma_2=1\times10^{5}; \gamma_3=1\times10^{-5}$ $; q=1\times10^{7}; r=1\times10^{-8};$

$$\dot{x}(t)=A_1x(t)+B_1u(t)+D_1\omega(t)$$
$$y(t)=C_1x(t)+D_2\omega(t) \qquad (7)$$

where x, u, y and ω are the state vector, system input, measured output and Gaussian white noise disturbance respectively; A_1, B_1, and C_1 state the system, input and output matrix respectively; while D_1 and D_2 are the system noise matrices. The cost function for the LQG controller is,

$$J=\lim_{T\to+\infty}E\left[\frac{1}{T}\int_0^T(x(t)^TQx(t)+u(t)^TRu(t))dt\right] \qquad (8)$$

Here, the symmetric weighting matrices are $Q \geq 0$ and $R > 0$, and the expected value is E. In Eq. (8), the term x^TQx represents the minimization of the states and the term u^TRu describes the minimization of the size of control inputs for the system. An integral action is included that minimizes the error. The updated plant is,

$$\dot{x}_f(t)=A_2x_f(t)+B_2u(t)+B_2\omega_1$$
$$z_f(t)=C_2x_f(t)+v \qquad (9)$$

Here, $v=[\omega_2 \quad \omega_3]^T$ is the augmented state, $x_f=[x \quad \int ydt]^T$ and $z_f=[z_1 \quad z_2]^T$ are the output vectors. For updated plant,

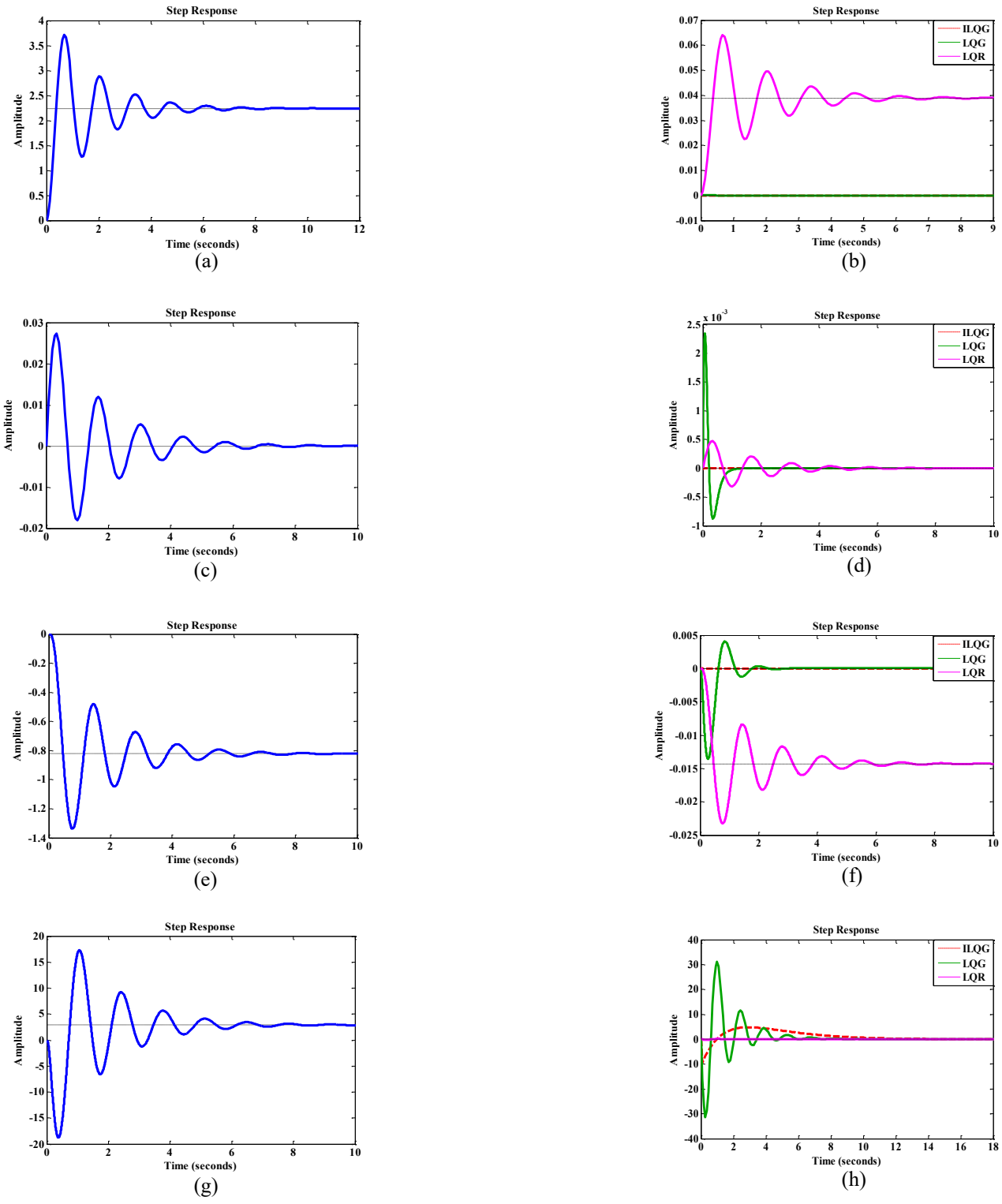

Fig. 5: Deviation of (a) Open-loop Rotor Angle, (b) Closed-loop Rotor Angle (c) Open-loop Speed, (d) Closed-loop Speed (e) Open-loop Terminal Voltage, (f) Closed-loop Terminal Voltage (g) Open-loop Exciter Voltage, (h) Closed-loop Exciter Voltage. Open-loop Response is Represented by Blue (-) Line. Green (-) Line, Magenta (-) Line and Red (- -) Dashed Line Represent the Closed-Loop Response of the LQG, LQR and ILQG Controller Respectively.

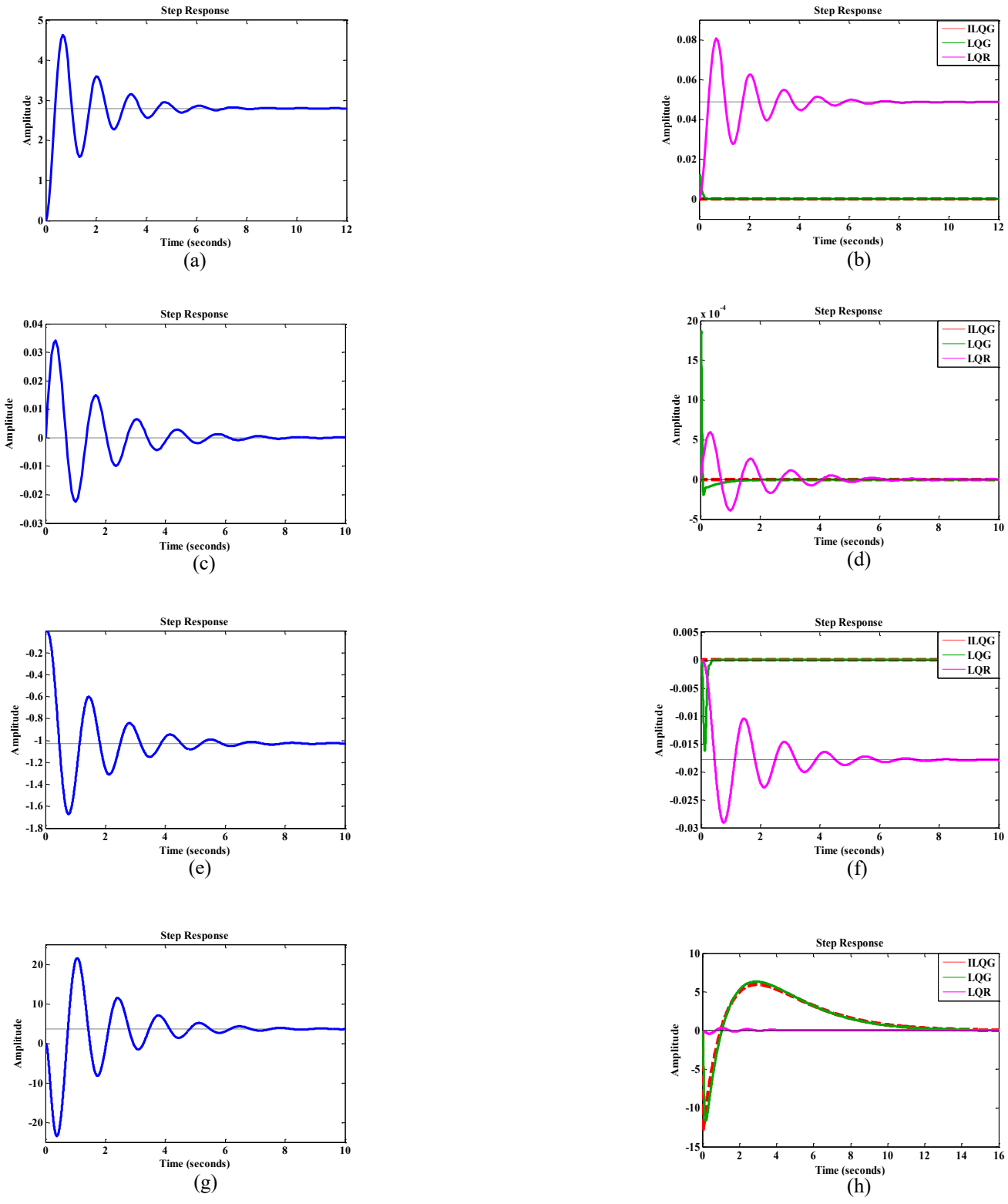

Fig. 6: Deviation of (a) Open-loop Rotor Angle, (b) Closed-loop Rotor Angle (c) Open-loop Speed, (d) Closed-loop Speed (e) Open-loop Terminal Voltage, (f) Closed-loop Terminal Voltage (g) Open-loop Exciter Voltage, (h) Closed-loop Exciter Voltage. Open-loop Response is Represented by Blue (-) Line. Green (-) Line, Magenta (-) Line and Red (- -) Dashed Line Represent the Closed-Loop Response of the LQG, LQR and ILQG Controller Respectively against Uncertainty.

Table 2. Closed-loop Step Response Comparison

Performance	ILQG Controller	LQG Controller	LQR Controller
Rotor Angle Deviation (s)	0.0197	1.19	6.19
Speed Deviation (s)	0.0195	0.02	6.56
Terminal Voltage Deviation (s)	0.132	2.13	6.31
Exciter Voltage Deviation (s)	10.01	6.89	2.12

$A_2 = \begin{bmatrix} A_1 & 0 \\ C_1 & 0 \end{bmatrix}$, $B_2 = \begin{bmatrix} B_1 \\ 0 \end{bmatrix}$ and $C_2 = \begin{bmatrix} C_1 & 0 \\ C_1 & I \end{bmatrix}$

where A_1 , B_1 and C_1 are defined in Eq. (7). Now ω_1 is the mechanical noise with variance ${\gamma_1}^2$, ω_2 is the sensor noise with variance ${\gamma_2}^2$ and ω_3 is the integral output sensor noise. Both are assumed as Gaussian white noise. The updated cost function based on Eq. (9) can be represents as,

$$J = \lim_{T\to+\infty} E\{\frac{1}{T}\int_0^T (x\ (t)^T Qx(t) + f(y)^T Q_I f(y) + u\ (t)^T Ru(t))dt\}$$

where $f(y)$ is state weighting matrices equal to $\int_0^T y(\tau)d\tau$ and $Q_I \geq 0$ is an integral state weighting matrices. Now, the ILQG controller can be given as,

$$\dot{\tilde{x}}_f(t) = A_2 \tilde{x}_f(t) + B_2 u(t) + K\ (z_f - C_2 \tilde{x}_f) \quad (10)$$

$$u(t) = -L\tilde{x}_f .$$

Here, K is the Kalman gain such as,

$K = P_K C_2^T R_K^{-1}$

Where P_K can be calculated using Riccati equation:

$$\tilde{P}_k = A_2 P_K + P_K A_2^T - P_K C_2^T R_K^{-1} C_2 P_K + Q_K$$

Here, $Q_K \geq 0$ and $R_K > 0$ are process and measurement noise matrices given by,

$$Q_K = {\gamma_1}^2 \ ; \ R_K = \begin{bmatrix} {\gamma_2}^2 & 0 \\ 0 & {\gamma_3}^2 \end{bmatrix}$$

Table 3. Closed-loop Step Response Comparison against Uncertainty

Performance	ILQG Controller	LQG Controller	LQR Controller
Rotor Angle Deviation (s)	0.0183	0.33	6.14
Speed Deviation (s)	0.00968	3.12	6.58
Terminal Voltage Deviation (s)	0.126	0.354	6.35
Exciter Voltage Deviation (s)	12.3	12.5	2.06

Where γ_1 is the standard deviation related to ω_1, γ_2 and γ_3 are the standard deviation related to ω_2 and ω_3 respectively. The gain L in Eq. (10) is given by,

$L = R_C^{-1} B_2 P_C$

where $P_C \geq 0$ can be calculated using Riccati equation,

$$\tilde{P}_C = A_2 P_C + P_C A_2^T - P_C C_2^T R_C^{-1} C_2 P_C + Q_C$$

Here, R_C is the weighting matrix of the controller and

$$Q_C = C_2{}^T \begin{bmatrix} 1 & 0 \\ 0 & q \end{bmatrix} C_2 .$$

The controller design parameters γ_1 , γ_2 , γ_3 , r and q are adjusted to achieve desired performance.

4. Performance Evaluation

The performance of SMIB is evaluated in this section under the proposed, LQR and LQG controller. MATLAB simulation is used as a tool to exam the performance of the SMIB. The parameters value of ILQG, LQG and LQR controller are listed in Table 1. Fig. 5(a), 5(c), 5(e) and 5(g) represent the open-loop performances of SMIB i.e. the deviation of rotor angle, speed, terminal voltage and exciter voltage of the generator. These results indicate that the performances are deviated from the desired result for insufficient damping torque of the induction machine. These deviations are reduced by using ILQG, LQG and LQR controllers are shown in Fig. 5(b), 5(d), 5(f) and 5(h).

The performance of SMIB is also investigated against uncertainty. Fig. 4 represents multiplicative output uncertainty where $G(s)$ represents system transfer function and $W(s)$ or $\delta(s)$ is the model variation. The selection of the value of $W(s)$ or $\delta(s)$ is in such way that can produce 25%

Table 4. Highlights of the ILQG, LQG and LQR Controller

Name of the Controllers	Advantages	Limitations
ILQG Controller	(i) High band-width, (ii) Large gain- and phase-margin, (iii) Robust, (iv) Track reference signal	-
LQG Controller	(i) High band-width,	(i) Can not track reference signal
LQR Controller	(i) High band-width,	(i) Can not track reference signal, (ii) Low operating region

variation of the reference signal. The open-loop response against uncertainty is represented in Fig. 6(a), 6(c), 6(e) and 6(g). The controlled performances are shown in Fig. 6(b), 6(d), 6(f) and 6(h) using ILQG, LQG and LQR controller. The controllers reduce these deviations to almost zero and make the system stable and reliable.

The comparative analysis between ILQG, LQG and LQR is investigated in this section which is used to find most optimum control algorithm for SMIB. Table 2 represents the comparison of settling time of ILQG, LQG and LQR controller. The settling time for rotor angle, speed and terminal voltage deviation are 0.0197s, 0.0195s and 0.132s respectively that are much lower as compare to LQG and LQR controller. Again, Table 3 represents the comparison of these controllers against uncertainty. Table 2 and Table 3 are the evidence that the settling time for ILQG controller is much lower as compared to the LQG and LQR controller. The results ensure that the ILQG controller is the most optimum controller that provides most robust performance.

5. Conclusion

The stability analysis of interconnected power system is quite challenging due to its complex characteristics and the effect of dynamic loads and uncertainties. The damping torque is an important factor that regains the proper rotor angle and speed of the generators by synchronizing them. The presence of any fault or uncertainty are responsible to reduce this damping torque that hampers the stability and robustness of the power system. The design of novel ILQG controller is presented in this paper to control the performances of SMIB such as the rotor angle, speed and voltage deviation by increasing the damping torque. To ensure the better performance of the proposed controller, a comparative analysis is investigated between the ILQG, LQR and LQG controller. The ILQG controller is efficiently able to reduce the oscilllations of the power system and help the system to regain sufficient dampind torque. The ILQG controller has settling time as 0.0197s, 0.0195s and 0.132s for rotor angle, speed and terminal voltage deviation without uncertainties which are much lower as compared to the LQG and LQR controller. Again, the deviation of these performances against uncertainty for ILQG controller are also smaller as compared to the LQG and LQR controller. The main limitation of the ILQG controller is that it can not properly control the exciter voltage deviation of SMIB. Table 4 summarizes these controller based on their advantage and limitation. The results and Table 4 ensure better control performance of the ILQG controller as compared to the LQR and the LQG controller that provides robust control of the SMIB against different uncertainties and fault.

6. Appendix

6.1 Power System Parameters

Generator: $M = 2H = 7, \tilde{\omega}_0 = 314, D = 0$, $x_d = 1.752 pu$, $\tilde{x}_d = 0.45 pu$, $T_d = 7.27 s$.

Exciter: $K_A = 200, T_A = 0.02$, $K_1 = 0.8645$, $K_2 = 0.8645$, $K_3 = 0.3135$, $K_4 = 1.4190$ $K_5 = 0.1465$, $K_6 = 0.4168$, $T_1 = 0.155$, $T_2 = 0.034$

References

[1] S. Gupta and R. K. Tripathi, “Transient Stability Enhancement of Multimachine Power System Using Robust and Novel Controller Based CSC-STATCOM,” *Advances in Power Electronics*, vol. 2015, 2015.

[2] Badal, Faisal R., Purnima Das, Subrata K. Sarker, and Sajal K. Das. "A survey on control issues in renewable energy integration and microgrid." *Protection and Control of Modern Power Systems 4*, no. 1 (2019).

[3] R. Ortega, M. Galaz, A. Astolfi, Y. Sun, and T. Shen, “Transient Stabilization of Multimachine Power Systems with Nontrivial Transfer Conductances,” *IEEE Transactions on Automatic Control*, vol. 50, no. 1, pp. 60 75,2005.

[4] P. Kethavath, “Transient Stability Analysis for Power System Networks with Asynchronous Generation,” Ph.D. dissertation, ResearchSpace@ Auckland, 2015.

[5] J. Ritonja, M. Petrun, J. Cernelic, R. Brezovnik, and B. Polajzer, “Analysis and Applicability of Heffron-Phillips Model,” *Elektronika ir Elektrotechnika*, vol. 22, no. 4, pp. 3–10,2016.

[6] Buccella, Concettina, Maria Gabriella Cimoroni, and Carlo Cecati. "Low-Frequency Harmonic Elimination Technique in Cascaded H-Bridges Multilevel Inverters

for Renewable Energy Applications." *International Journal of Smart Grid-ijSmartGrid3*, no. 1 (2019): 1-9.

[7] Harrouz, Abdelkader, Meriem Abbes, Ilhami Colak, and Korhan Kayisli. "Smart grid and renewable energy in Algeria." *In 2017 IEEE 6th International Conference on Renewable Energy Research and Applications (ICRERA),* pp. 1166-1171. IEEE, 2017.

[8] M. S. Shahriar, M. A. Ahmed, and M. S. Ullah, "Design and Analysis of a Model Predictive Unified Power Flow Controller (MPUPFC) for Power System Stability Assessment," *International Journal of Electrical & Computer Sciences IJECS-IJENS*, vol. 12, no. 04, 2012.

[9] Sarkar, Subrata K., Md Hassanul K. Roni, D. Datta, Sajal K. Das, and Hemanshu R. Pota. "Improved design of high-performance controller for voltage control of islanded microgrid." *IEEE Systems Journal 99* (2018): 1-10.

[10] Rahman, Mizanur, Subroto K. Sarkar, Sajal K. Das, and Yuan Miao. "A comparative study of LQR, LQG, and integral LQG controller for frequency control of interconnected smart grid." *In2017 3rd International Conference on Electrical Information and Communication Technology (EICT),* pp. 1-6. IEEE, 2017.

[11] S. Latha, M. R. Slochanal, and J. P. Rajan, "Stability Analysis of Single Machine Infinite Bus Power System with TCSC Controller," *Data Mining and Knowledge Engineering*, vol. 2, no. 11, pp. 354–359, 2010.

[12] D. K. Sambariya and R. Prasad, "Design of Optimal Proportional Integral Derivative Based Power System Stabilizer Using Bat Algorithm," *Applied Computational Intelligence and Soft Computing*, vol. 2016, p. 5, 2016.

[13] Siddique, Abu Bakar, Md Shahin Munsi, Subrata K. Sarker, Sajal K. Das, and Md Rabiul Islam. "Voltage and current control augmentation of islanded microgrid using multifunction model reference modified adaptive PID controller." *International Journal of Electrical Power & Energy Systems 113 (2019)*: 492-501.

[14] Rahman, Md Arifur, Subrata K. Sarkar, Faisal R. Badal, and Sajal K. Das. "Optimal Design of Integral Linear Quadratic Gaussian Controller for Controlling of Islanded Microgrid Voltage*." In 2018 International Conference on Advancement in Electrical and Electronic Engineering (ICAEEE),* pp. 1-4. IEEE, 2018.

[15] S. A. S. O. Al-Kadhim, "Simulation of Multi-Machine Transient Stability," Ph.D. dissertation, Ministry of Higher Education, 2010.

[16] M. Mahmud, "An Alternative LQR-Based Excitation Controller Design for Power Systems to Enhance Small-Signal Stability," *International Journal of Electrical Power & Energy Systems*, vol. 63, pp. 1–7, 2014.

[17] S. Panda and N. P. Padhy, "MATLAB/SIMULINK Based Model of Single-Machine Infinite-Bus with TCSC for Stability Studies and Tuning Employing GA," *International journal of Computer science and Engineering*, vol. 1, no. 1, pp. 50–59, 2007.

[18] B. S. Surjan and R. Garg, "Power System Stabilizer Controller Design for SMIB Stability Study," *International Journal of Engineering and Advanced Technology (IJEAT) ISSN*, pp. 2249–8958, 2012.

[19] W. Dib, R. Ortega, A. Barabanov, and F. Lamnabhi-Lagarrigue, "A "Globally" Convergent Controller for Multi-Machine Power Systems Using Structure-Preserving Models," *IEEE Transactions on Automatic Control*, vol. 54, no. 9, pp. 2179–2185, 2009.

[20] A. Giusto, R. Ortega, and A. Stankovic, "On Transient Stabilization of Power Systems: A Power-Shaping Solution for StructurePreserving Models," in *Decision and Control, 2006 45th IEEE Conference on*. IEEE, 2006, pp.4027–4031.

[21] D. Casagrande, A. Astolfi, R. Ortega, and D. Langarica, "A Solution to the Problem of Transient Stability of Multimachine Power Systems," in *Decision and Control (CDC), 2012 IEEE 51st Annual Conference on*. IEEE, 2012, pp. 1703–1708.

[22] S. Paliwal, P. Sharma, and A. K. Sharma, "Dynamic Stability Enhancement of Power System Using Intelligent Power System Stabilizer," in *Proceedings of Fourth International Conference on Soft Computing for Problem Solving*. Springer, 2015, pp. 571–583.

[23] R. Patel, T. Bhatti, and D. Kothari, "Study of Power System Transient Stability with Simulink."

[24] A. Kharrazi, "Tuning of Power System Stabilizer in Single Machine Infinite Bus (SMIB) Using Genetic Algorithm and Power Factory Modal Analysis," in *Power Engineering Conference (AUPEC), 2015 Australasian Universities*. IEEE, 2015, pp. 1–6.

[25] Wang, Yanbo, Dong Liu, Zhe Chen, and Ping Liu. "A hierarchical control strategy of microgrids toward reliability enhancement." *In 2018 International Conference on Smart Grid (icSmartGrid),* pp. 123-128. IEEE, 2018.

[26] Tur, Mehmet Rida, İlhami Colak, and Ramazan Bayindir. "Effect of Faults in Solar Panels on Production Rate and Efficiency." *In 2018 International Conference on Smart Grid (icSmartGrid),* pp. 287-293. IEEE, 2018.

[27] Muljadi, Eduard, Woonki Na, Bill Leighty, and Jonghoon Kim.Control and Analysis for a Self-Excited Induction Generator for Wind Turbine and Electrolyzer Applications. No. NREL/CP-5D00-71219. *National*

Renewable Energy Lab.(NREL), Golden, CO (United States), 2017.

[28] Sarkar, Subroto K., Faisal R. Badal, and Sajal K. Das. "A comparative study of high performance robust pid controller for grid voltage control of islanded microgrid." *International Journal of Dynamics and Control 6*, no. 3 (2018): 1207-1217.

[29] Sikder, Stanley H., Md Mukidur Rahman, Subrata K. Sarkar, and Sajal K. Das. "Fractional order robust pid controller design for voltage control of islanded microgrid." *In 2018 4th International Conference on Electrical Engineering and Information & Communication Technology (iCEEiCT),* pp. 234-239. IEEE, 2018.

[30] Armin, Maniza, Priyo Nath Roy, Subroto K. Sarkar, and Sajal K. Das. "LMI-based robust PID controller design for voltage control of islanded microgrid." *Asian Journal of Control 20*, no. 5 (2018): 2014-2025.

[31] V. Bandal, B. Bandyopadhyay, and A. Kulkarni, "Output Feedback Fuzzy Sliding Mode Control Technique Based Power System Stabilizer (PSS) for Single Machine Infinite Bus (SMIB) System," in *Industrial Technology, 2005. ICIT 2005. IEEE International Conference on*. IEEE, 2005, pp. 341–346.

[32] Lazaroiu, Cristian, Mariacristina Roscia, and Dario Zaninelli. "Fuzzy Logic to Improve Prosumer Experience into a Smart City." *In 2018 International Conference on Smart Grid (icSmartGrid),* pp. 52-57. IEEE, 2018.

[33] E. Afzalan and M. Joorabian, "Analysis of the Simultaneous Coordinated Design of STATCOM-based Damping Stabilizers and PSS in a Multi-machine Power System Using the Seeker Optimization Algorithm," *International Journal of Electrical Power & Energy Systems*, vol. 53, pp. 1003–1017, 2013.

[34] M. Shirvani, A. A. D. Mostafa Abdollahi, and I. Baghbani, "Application of Cultural Algorithm to Adjust the Supplementary Stabilizer of STATCOM," *International Journal of Academic Research*, vol. 6, no. 4, 2014.

[35] M. A. Mahmud, H. Pota, and M. Hossain, "Nonlinear DSTATCOM Controller Design for Distribution Network with Distributed Generation to Enhance Voltage Stability," *International Journal of Electrical Power and Energy Systems*, vol. 53, pp. 974–979, 2013.

[36] Y. Ni, Z. Huang, S. Chen, and B. Zhang, "Incorporating UPFC Model into the Power System Toolbox of the MATLAB for Transient Stability Study," in *TENCON'98. 1998 IEEE Region 10 International Conference on Global Connectivity in Energy, Computer, Communication and Control*, vol. 2. IEEE, 1998, pp. 506–509.

[37] Sarkar, Subroto K., Faisal R. Badal, Sajal K. Das, and Yuan Miao. "Discrete time model predictive controller design for voltage control of an islanded microgrid." *In 2017 3rd International Conference on Electrical Information and Communication Technology (EICT),* pp. 1-6. IEEE, 2017.

[38] Rahman, Mizanur, Subrata K. Sarker, Sajal K. Das, and M. F. Ali. "Model Predictive Control Framework Design for Frequency Regulation of PREYs Participating in Interconnected Smart Grid." *In 2019 International Conference on Electrical, Computer and Communication Engineering (ECCE),* pp. 1-6. IEEE, 2019.

[39] H. Ko, K. Lee, and H. Kim, "An Intelligent Based LQR Controller Design to Power System Stabilization," *Electric Power Systems Research*, vol. 71, no. 1, pp. 1–9, 2004.

[40] S. Ganjefar and A. Judi, "Centralized Optimal Control for a Multimachine Power System Stability Improvement Using Wave Variables," *International Journal of Recent Trends in Engineering*, vol. 1, no. 3, p. 63, 2009.

[41] Y. Wang, G. Guo, and D. J. Hill, "Robust Decentralized Nonlinear Controller Design for Multimachine Power Systems," *Automatica*, vol. 33, no. 9, pp.1725–1733, 1997.

[42] S. Duman and A. Ozt ¨ urk, "Robust Design of PID Controller for Power System Stabilization by Using Real Coded Genetic Algorithm," ¨ *International Review of Electrical Engineering*, vol. 5, no. 5, pp. 2159–2170, 2010.

[43] Rahman, Mizanur, Subrata K. Sarkar, and Sajal K. Das. "Stabilization Improvement of Load Frequency Deviation for Multi-Area Interconnected Smart Grid Using Integral Linear Quadratic Gaussian Control Approach." *In 2018 10th International Conference on Electrical and Computer Engineering (ICECE),* pp. 477-480. IEEE, 2018.

[44] Badal, Faisal R., Subrata K. Sarkar, and Sajal K. Das. "High Performance ILQG Controller Design to Enhance Dynamic Stability of Multimachine Power System." *In 2018 4th International Conference on Electrical Engineering and Information & Communication Technology (iCEEiCT),* pp. 142-147. IEEE, 2018.